AIAA JOURNAL
Vol. 42, No. 7, July 2004

Buckling Response of Transversely Loaded Composite Shells, Part 2: Numerical Analysis

Brian L. Wardle,* Paul A. Lagace,† and Mark A. Tudela‡
Massachusetts Institute of Technology, Cambridge, Massachusetts 02139

The response of transversely point-loaded composite shells is investigated via the finite element method. The thin, circular cylindrical shells are hinged at a fixed distance apart on the straight edges and are free on the curved edges. Stability issues are considered, including nonlinear prebuckling, limit points, bifurcation, and postbuckling. In the finite element formulation, a novel technique is utilized to identify and traverse bifurcation points efficiently in the nonlinear elastic response. A classic shell buckling benchmark problem is solved here correctly for the first time; previous studies have found the isotropic shell to have a limit point, when, in fact, the shell bifurcates before reaching a limit point. Predicted results for graphite/epoxy laminated shells are in excellent agreement with measured load-deflection and mode-shape evolutions as previously reported. Two cases of extraordinarily good agreement between the data and model, particularly large-deflection asymmetric deformations modes through a bifurcation point and far into the postbuckling regime, clearly establish validated new benchmarks. Asymmetries in both directions of the shell plane, relative to the centrally applied point load, are discussed with regard to bifurcation and material couplings in the composite laminate. Asymmetric stress distributions are discussed in the context of composite damage resistance and previous experimental findings on atypical shell damage mode and extent. The influence of test fixture compliance is evaluated and briefly discussed.

I. Introduction

LAMINATED composites continue to see increased use in high-performance, weight-critical applications, for example, the hydrogen fuel tank in next-generation reusable launch vehicles,[1] due to performance advantages over traditional metallic materials. Advantages of composites include high specific stiffness and strength, excellent fatigue characteristics, environmental properties, (for example, high operating temperatures), and mechanical tailoring capabilities. Unfortunately, widespread composites usage has been deterred by damage and fracture issues, particularly impact damage resistance/tolerance concerns in the aerospace industry. For example, performance reductions, in this case static strength, of greater than 50% have been correlated with barely visible impact damage (BVID).[2–4] Concerns such as these have driven extensive investigations into impact damage of composite structures, primarily plates, and several review papers[4–6] have appeared. One significant finding with regard to impact is that quasi-static testing oftentimes gives an equivalent response, including damage state.[7–14] This is particularly true of composite shells such as those considered in this work[15] where the mode and extent of damage are known to be equivalent. Thus, quasi-static testing can simulate impact loading. The static response then becomes the focus of investigations striving to understand the impact response.

Calculation of the structural response of transversely loaded composite shells requires significant computational effort due to nonlinear geometric/kinematic couplings, large rotations, and buckling. Analytical and numerical studies, particularly finite element analyses, have sought to characterize the structural response of composite shells to static transverse loading (for example, Refs. 16–21) and also to impact (for example, Refs. 18 and 21–25). The existence of a shell buckling instability results in (oftentimes drastic) differences in structural and damage response compared to plates.[18,23,26–32] Arches display similar response characteristics,[33,34] and results from arch analyses are useful to obtain a qualitative understanding of shell buckling response. Nonlinear collapse at a limit point or bifurcation buckling[35] is often the dominant mode of failure for thin shell structures, and both cases must be considered in any analysis. Bifurcation presents additional challenges (such as identification of bifurcation points and switching to the secondary path) for finite element analyses, particularly when nonlinear prebuckling exists. Previous finite element analyses have found the limit-point response, effectively ignoring bifurcation, by imposition of quarter-models due to assumed symmetries.[16–18,20,21,24,26,36–44] However, finite element analyses with these assumptions cannot capture the asymmetric bifurcation observed in Part 1 (Ref. 45) of this work and, thus, will not give an accurate prediction of the shell response.

The objective of the present work is to investigate shell buckling response under centered, transverse point-loading by the use of the finite element method. Particularly, two significant issues in the shell response that have not been previously addressed are considered: bifurcation buckling and experimental correlation(s) of the finite element analyses. Bifurcation from the nonlinear prebuckling state is incorporated into the finite element analyses by the use of a novel asymmetric meshing technique (AMT). This technique has been previously presented[46] and is illustrated here using a benchmark isotropic shell problem from the literature.[47] Finite element results are compared to experimental load-deflection and mode-shape data[32] for the composite shells described in Part 1 (Ref. 45). Of particular importance is the calculation of the bifurcation load/mode that has not been previously reported for these shell structures. The effect(s) of test fixture compliance on the composite shell behavior are also considered. Insights from the experimental/numerical comparisons and implications for damage resistance, particularly observed asymmetric and atypical damage states, are discussed.

II. Approach

The elastic response of transversely loaded composite shells is investigated in this work by the use of finite elements. The shells are statically center loaded with boundary conditions of pinned/no in-plane sliding, that is, hinged, along the straight circumferential

Received 20 March 2002; revision received 28 August 2003; accepted for publication 30 January 2004.

*Boeing Assistant Professor, Technology Laboratory for Advanced Composites, Department of Aeronautics and Astronautics. Member AIAA.

†Professor and MacVicar Faculty Fellow, Technology Laboratory for Advanced Composites, Department of Aeronautics and Astronautics. Associate Fellow AIAA.

‡Graduate Student, Technology Laboratory for Advanced Composites, Department of Aeronautics and Astronautics; currently Research Aerospace Engineer, U.S. Air Force Materials Laboratory, 2941 P. Street, Wright–Patterson Air Force Base, OH 45433.

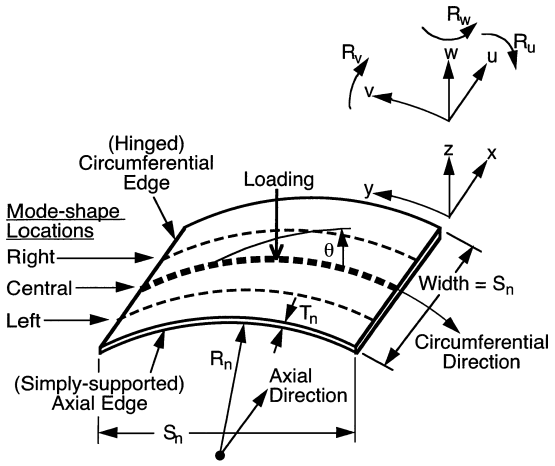

Fig. 1 Generic shell specimen with ply orientation and geometric variables R_n (radius), S_n (span), and T_n (thickness); boundary conditions, displacements, and rotations used in the finite element analysis and mode shape locations are also indicated.

edges and free along the curved axial edges (Fig. 1). Specifics of the modeling assumptions, particularly in regard to the experiments, are detailed in the next section. Refer to the experimental paper[45] for details of the experiments and composite shell configurations.

A benchmark isotropic shell problem[47] for large rotations/deflections is first evaluated to illustrate typical behavior of shells in this work. The limit-point solution often found in the literature is solved by the use of the nonlinear features of the STAGS finite element code[48] and compared to the bifurcation solution obtained with the new technique. The benchmark solutions identify both the importance of bifurcation and also the utility of the novel asymmetric meshing technique. Next, both limit-point and bifurcation solutions are computed for each of the composite shells tested in Part 1 (Ref. 45). Comparisons are made to validate the analyses based on measured load-deflection data and mode-shape evolutions. The load-deflection data allow an average structural response comparison, whereas the deflection mode shapes give additional insight into the shell buckling mechanism, particularly whether or not bifurcation occurs. The detailed finite element results elucidate the experimental findings and contribute to a better overall understanding of the buckling and postbuckling behavior of composite shells.

III. Finite Element Modeling

The STAGS finite element code[48] is used to analyze the elastic response of transversely (center) loaded shells. This code is used extensively to analyze the nonlinear response of (composite) shell structures. The 410-shell element available in STAGS is utilized for its applicability to the thin shell structures in this work (see Ref. 49). This "workhorse" element in the STAGS code employs the nonlinear Kirchhoff–Love shell hypothesis, which ignores transverse shear. However, it is known to be extremely accurate for modeling thin shell structures. It is a displacement-based four-node quadrilateral C^1 shell element having a cubic (translations and rotations) bending field and a linear/cubic (in-plane translation/transverse rotations) membrane field. The 410-shell element has three translational and three rotational degrees of freedom per node and also includes drilling rotational stiffness. The true Newton capability is utilized to solve the resulting nonlinear equations iteratively. Arbitrarily large rotations, but small strains, are modeled by the use of the standard nonlinear corotational procedure[44] in STAGS, and limit points are traversed by use of the Riks arc-length procedure.[50]

The right-handed curvilinear coordinate system used in this work is shown for a generic shell in Fig. 1. In all cases, the boundary conditions are free of traction on the axial edges and hinged on the circumferential edges. The circumferential edge (hinged) constraint is represented in the model when all nodal displacements and rotations ($u = v = w = Rv = Rw$) are set equal to zero, except rotation about the x axis (Ru), where zero moment is enforced. In the analysis, the shells are transversely point-loaded in all cases at the center of the shell surface. Quarter-symmetry was not assumed because a full model of the shell is required to investigate bifurcation.

The novel approach for inducement of bifurcation used in this work arises from the consideration of traditional techniques, particularly the effects imperfections have on the finite element model itself. Traditional techniques for inducement of bifurcation all involve the introduction of perturbations into the numerical model through the stiffness (or, more correctly, tangent stiffness) matrix via geometric imperfections or through the loading vector via loading imperfections. For example, the equivalence transform technique[48] in the STAGS code uses the eigenvector of the local bifurcation mode as an imperfection to perturb the numerical model. Perturbations due to this fictitious imperfection allow a transition to the secondary bifurcation path because this path is preferred as the lowest energy state. However, the mode(s) and corresponding amplitude(s) of the imperfection must be subjectively introduced into the analysis and, thus, require earlier knowledge, experience, and/or search techniques. Furthermore, such subjective choices result in different responses, sometimes with little relation to the actual problem being considered. In the current work, a numerical perturbation to the stiffness matrix is introduced when the structure is meshed asymmetrically. The resulting perturbed stiffness matrix in the nonlinear mathematical model acts to induce bifurcation in the same way as geometric and loading imperfections in the traditional techniques. This AMT succeeds in perturbing the numerical model without altering the problem being considered, that is, no imperfections are introduced. This allows the bifurcation response of the structure (including postbuckling), if it exists, to be obtained directly. A complete discussion of the AMT is presented in Ref. 46.

A typical asymmetric mesh used in this work is presented in Fig. 2. The shell is divided into two shell units with different mesh densities and can be contrasted to a typical 10 by 10 symmetric mesh. The first shell unit covers 60% of the shell in the circumferential (y) direction, whereas the second shell unit covers the remaining 40%. The first 60% of the shell (first shell unit) is meshed identically to the 10 by 10 symmetric mesh with six elements along the curved surface. The second 40% of the shell (second shell unit) contains five, rather than four, elements in the circumferential direction. This creates an asymmetric mesh with 11 elements (total) in the circumferential direction and 110 elements to represent the entire shell. This distribution, rather than a 50%/50% division, was originally used to avoid application of the point load along the interface of the two shell units. Subsequent analyses with various distributions show that this conservatism was not necessary.[46] Discretization is denoted in this work by a list of the number of elements in the axial (x) direction and circumferential (y) directions for 60 and 40% of the shell circumference, respectively. A symmetric mesh of 100 elements is denoted by a $10 \times 6/10 \times 4$ mesh, whereas the asymmetric mesh of 110 elements described earlier is denoted by a $10 \times 6/10 \times 5$ mesh.

Full details of the experiments analyzed in this work can be found in Part 1 (Ref. 45). The composite shells tested (in Ref. 45) were manufactured from Hercules AS4/3501-6 graphite/epoxy prepreg

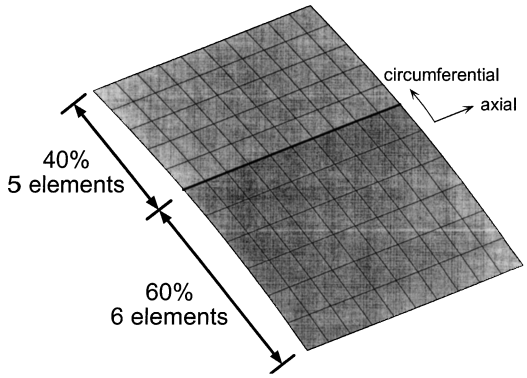

Fig. 2 Asymmetrically meshed shell discretized into two shell units in the circumferential (y) direction.

Table 1 AS4/3501-6 ply material properties

Property	Value
E_{11}	142 GPa
E_{22}	9.81 GPa
G_{12}	6.00 GPa
ν_{12}	0.30
Ply thickness	0.134 mm

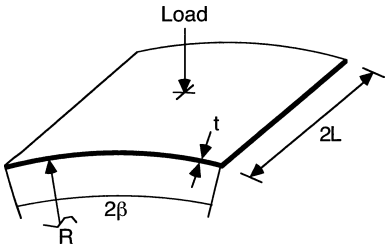

Fig. 3 Geometry and material data for benchmark shell problem.[47] Center load square planform, $L = 254$ mm, $R = 2540$ mm, $t = 6.35$ mm, $\beta = 0.1$ rad, $E = 3.10275$ GPa, and $\nu = 0.3$.

tape in a $[\pm 45_n/0_n]_s$ layup where $n = 1$, 2, and 3 (Ref. 32). Ply material properties used in the analysis are given in Table 1. Effective laminate properties are computed within STAGS based on these ply properties. Structural parameters and the orientation of ply angle θ with respect to the specimen axes are identified in Fig. 1. Experimental values of radius[32] are used in the analysis, whereas nominal values are used for span and laminate/ply thickness. Nominal base values X_1 for each of the structural parameters are R_1 equal to 152 mm (6 in.) for radius, S_1 equal to 102 mm (4 in.) for span, and T_1 equal to 0.804 mm (6 plies) for thickness. Specimens are designated as in Ref. 45 with subscripts indicating scale factors for the base values: $X_n = n(X_1)$. The shells were loaded with a 12.7-mm ($\frac{1}{2}$-in.)-diam hemispherical steel indentor at the center of the shell. This is idealized as a point load at the shell center in the analyses. The path-parameter (Riks arc-length) method is used to increment the loading in the analyses. This also differs from the experiments wherein the load was introduced under displacement (stroke) control. A mesh of $30 \times 12/30 \times 9$ is utilized to generate smooth deflection mode shapes in both the axial and circumferential directions for comparison to the experimental data. Experimental boundary conditions are idealized as hinged on the circumferential edges and free on the axial edges, as discussed earlier. Effects of loading and boundary condition idealizations are discussed in Sec. V.

IV. Benchmark Shell Problem

A benchmark shell problem from the literature[47] was first analyzed to illustrate typical shell response, including nonlinear prebuckling, nonlinear collapse (limit points), bifurcation, and postbuckling. Material and geometric properties for the benchmark problem are given in Fig. 3. Loading and boundary conditions are identical to those described for the experimental work.

The load-deflection response from the STAGS analysis for the benchmark isotropic shell problem is presented in Fig. 4, along with solutions from the literature for comparison.[43,47] Both load and deflection are taken positive in the loading direction shown in Fig. 3. The limit-point solution corresponds to a symmetric model with 10 elements in both the axial and circumferential directions. This rather coarse mesh represents a converged solution checked against a more refined 20 by 20 element mesh ($20 \times 12/20 \times 8$) and repeats the limit-point response found in the literature. The bifurcation solution corresponds to the asymmetric $10 \times 6/10 \times 5$ mesh.

The behavior of the benchmark shell (Fig. 4) serves to illustrate two typical buckling responses for point-loaded shells. In the case of the symmetric mesh and solutions from the literature, a limit point is reached and the shell buckles into a mode corresponding to the prebuckling behavior. The buckling mode is symmetric with respect to the loading in both the axial and circumferential directions. In the case of the asymmetric mesh, the response bifurcates into a mode that is asymmetric with respect to the loading in the circumferential (y in Fig. 1) direction. Traditional techniques for evaluation of bifurcation with finite elements confirm the bifurcation response and mode shapes generated by the AMT in Fig. 4 (Ref. 46). The limit-point and bifurcation responses are qualitatively similar to, respectively, the well-known extensional and inextensional deformation modes of one-dimensional shallow arches.[51] Because the critical load for the bifurcation is 12% below the limit-point collapse load, bifurcation represents the actual response of the shell. The limit-point solutions from the literature, including the snapback response often mentioned in relation to this problem, wherein both the load and deflection decrease simultaneously (Fig. 4), will never be realized because the lower-energy bifurcation path is preferred. The bifurcation and limit-point solutions converge on the symmetric postbuckled (final) equilibrium path as expected.

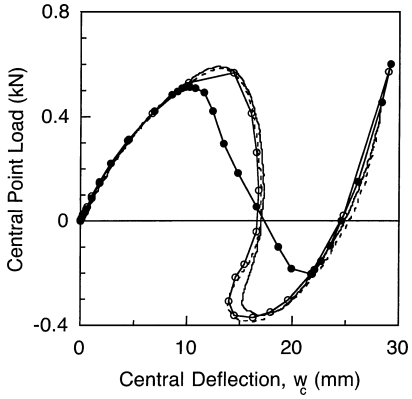

Fig. 4 Limit-point and bifurcation load-deflection paths for benchmark shell problem: ——, Sabir and Lock[47]; - - - - -, Crisfield[43]; ○, STAGS (limit point); and ●, STAGS (bifurcation).

V. Results and Discussion

As noted in Sec. II, both load-deflection and mode-shape data from the experiments described in Part 1 (Ref. 45) are available for comparison to the finite element results. Data are available only for positive loads due to characteristics of the experiments as described in Ref. 45. In addition to basic comparisons of numerical and experimental results, the influence of experimental realities (such as test-fixture compliance) and bending–twisting laminate coupling on the composite shell response are investigated.

A. Numerical/Experimental Comparisons

Detailed numerical comparisons to measured load-deflection and mode-shape evolutions for two composite shells ($R_6S_3T_1$ and $R_{12}S_3T_1$) are presented in this section. The location of the central spanwise mode shape is indicated in Fig. 1. As in the benchmark problem, both deflection and load are considered positive in the direction of load application (z direction in the coordinate system of Fig. 1). Displacement is nondimensionalized with respect to specimen thickness to emphasize the large-deflection nature of the shell behavior. All results represent converged solutions attained through mesh refinement studies. Such studies show that a $10 \times 6/10 \times 5$ mesh is adequate to capture the response, including bifurcation and postbuckling, of all composite shells considered. However, as indicated earlier, $30 \times 12/30 \times 9$ meshes are used so that smooth mode-shape plots can be generated for comparison to the experimental data. In addition to the mesh-refinement studies, all results generated with the AMT were verified by the use of traditional techniques for inducing bifurcation.[46]

Excellent agreement is obtained for the load-deflection response between the numerical solutions found with the AMT and the experimental data, as shown in Figs. 5 and 6. Both limit-point (symmetric mesh) and bifurcation (asymmetric mesh) solutions are provided in the load-deflection responses in Figs. 5 and 6 to emphasize the importance of the evaluation of bifurcation. Bifurcation is clearly

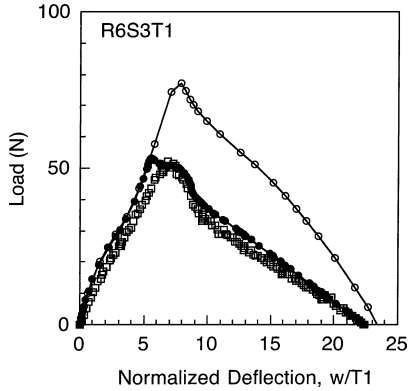

Fig. 5 Numerical and experimental[48] central load-deflection results for the transverse buckling response of a composite shell, specimen $R_6S_3T_1$, radius = 0.9124 m: ○, limit point; ●, bifurcation; and □, data.

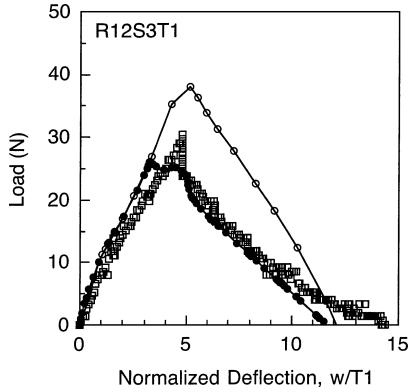

Fig. 6 Numerical and experimental[48] central load-deflection results for the transverse buckling response of a composite shell, specimen $R_{12}S_3T_1$, radius = 1.743 m: ○, limit point; ●, bifurcation; and □, data.

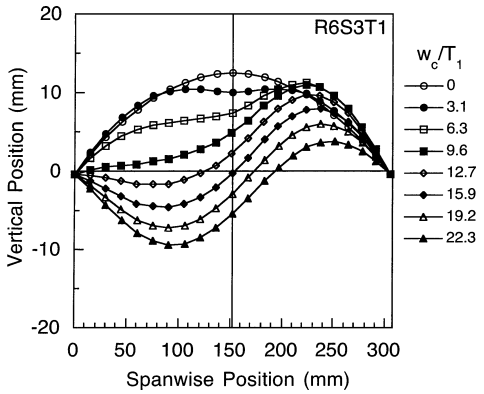

Fig. 7a Numerical results for central spanwise deformation modes for specimen $R_6S_3T_1$ at different normalized center deflections, w_c/T_1.

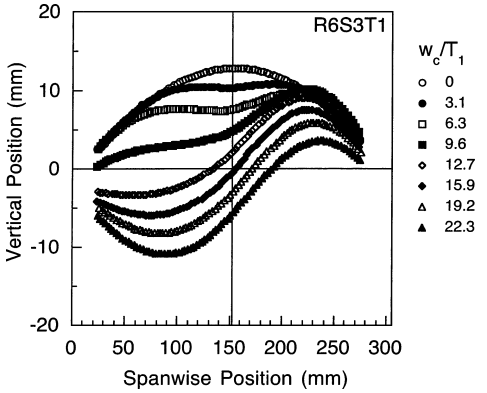

Fig. 7b Experimental results[48] for central spanwise deformation modes for specimen $R_6S_3T_1$ at different normalized center deflections, w_c/T_1.

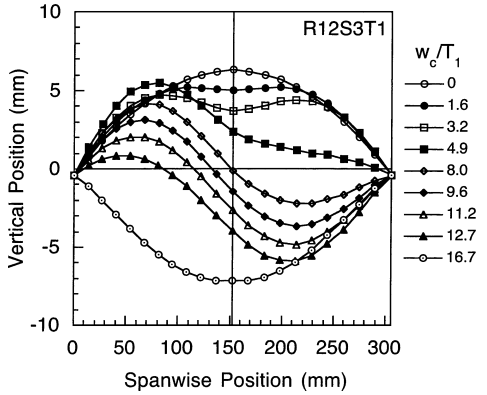

Fig. 8a Numerical results for central spanwise deformation modes for specimen $R_{12}S_3T_1$ at different normalized center deflections, w_c/T_1.

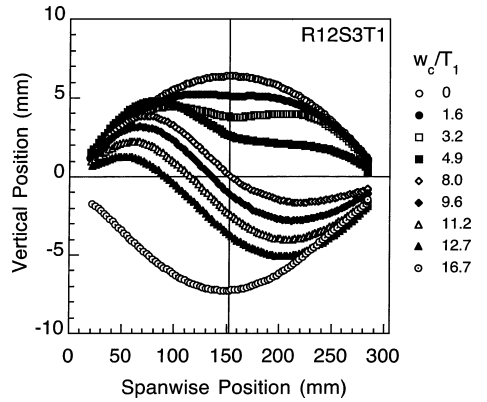

Fig. 8b Experimental results[48] for central spanwise deformation modes for specimen $R_{12}S_3T_1$ at different normalized center deflections, w_c/T_1.

the critical consideration in the response of these two shells, which buckle at 67% of the limit load in the numerical analysis, in agreement with the observed behavior.

Comparison of central spanwise mode-shape evolutions in Figs. 7 and 8 provide further evidence that the numerical results capture the experimental behavior. Mode shapes are provided in a global Cartesian reference frame, different than the curvilinear system in Fig. 1, at discrete values of nondimensional center deflection (w_c/T_n) to reference Figs. 5 and 6. Excellent agreement is noted in the mode-shape development at all values of applied center deflection (stroke) for both specimens in Figs. 7 and 8. Symmetric mode shapes are evident for displacements below the critical (bifurcation) point in both the numerical (Figs. 7a and 8a) and experimental results (Figs. 7b and 8b). A dominant asymmetric mode, with respect to the loading in the circumferential direction, is evident only after the critical point between nondimensional center deflections of 3.1 and 6.3 in Figs. 7. The same transition, from a primary symmetric mode before bifurcation to a dominant asymmetric mode, is also noted in the numerical and experimental response of specimen $R_{12}S_3T_1$ in Figs. 8 between nondimensional center deflections of 3.2 and 4.9. Bifurcation is easily identified in the mode-shape response as a dominant asymmetric mode following the critical point in the load-deflection response for these shells.

Central mode shapes in the axial direction for both specimens also reveal good agreement between numerical and experimental results, as seen in Figs. 9a and 9b for specimen $R_{12}S_3T_1$. Unlike the numerical results in Fig. 9a, the experimental data (Fig. 9b) indicate

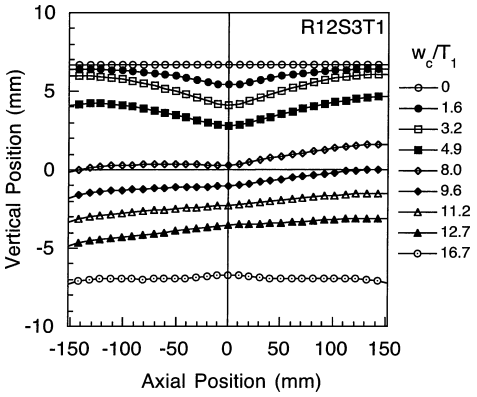

Fig. 9a Numerical results for central axial deformation modes for specimen $R_{12}S_3T_1$ at different normalized center deflections, w_c/T_1.

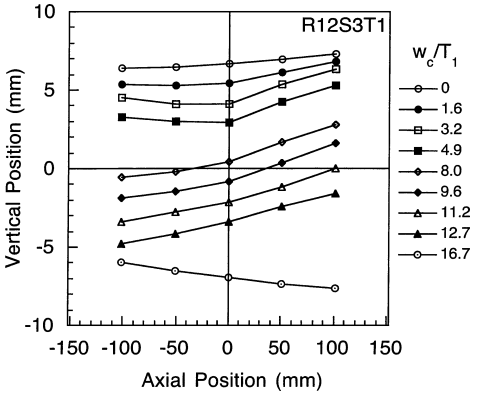

Fig. 9b Experimental results[48] for central axial deformation modes for specimen $R_{12}S_3T_1$ at different normalized center deflections, w_c/T_1.

some variation in the axial height of the undeformed specimen, likely due to gravity loading the shell transversely before any load is applied by the loading apparatus. This initial deviation in shell height is further evidenced in the subsequent mode shapes during loading. However, as shown by the excellent agreement between numerical and experimental results in Figs. 5 and 6, the initial deviation in shell height does not appear to affect the shell load-deflection response significantly. In general, excellent agreement between the numerical and experimental results are noted for both the axial and spanwise deformation modes of specimens $R_6S_3T_1$ and $R_{12}S_3T_1$.

Shell response in this work is sensitive to imperfections and other experimental realities, such as imperfect boundary conditions, indentation (contact behavior) at the loading point, and damage. These effects have not been accounted for in the elastic models in this work. Determination of the exact point of bifurcation from experimental load-deflection and mode-shape data is subjective because it involves judging an asymmetric mode from a symmetric one. However, in many of the cases, such as those presented thus far, it is clear that bifurcation occurs. In Part 1, one-half (9 of 18) of the shells tested are noted to bifurcate before reaching a limit point.[45] The finite element results are in good agreement with this observation because the analysis predicts these nine shells to bifurcate. Two additional shells are predicted to bifurcate, but did not exhibit bifurcation in the experimental results. The two specimens that do not bifurcate experimentally, $R_{12}S_3T_3$ and $R_6S_2T_3$, both exhibit strong elastic interaction with the test fixture. This is evident in the load-deflection plots for these two specimens and is considered in detail in the subsection on Experimental Realities in this work.

B. Two-Dimensional Shell Behavior

The predicted postbuckling load-deflection response immediately following bifurcation, shown in Figs. 5 and 6, contains several local minima and maxima that deserve further consideration. These local minima and maxima are not distinguishable in the experimental data. The majority of shells analyzed from Part 1 (Ref. 45) that bifurcate before reaching a limit point display this subtle behavior. "Snapback" behavior of the benchmark problem can be used to explain these local minima and maxima in the computed composite shell response. Snapback is commonly utilized to explain the counterintuitive region of the limit-point response (see Fig. 4) where both load and deflection decrease during loading (see, for example, Ref. 44). The snapback explanation holds that, in this region, the free shell edges snap through to an inverted (collapsed) configuration, whereas the shell center snaps back (decreased deflection). Snapback, thus, refers to the two-dimensional nature of the buckling response for these shells and is not a feature of one-dimensional arch response.

The two-dimensional nature of the composite shells studied in this work also implies that the response can, and does, vary significantly between the shell center and free edges (axial direction), that is, the shell does not deform as an arch. Axial variation in the deformation mode shapes is evident in the numerical results of the mode-shape evolutions compared in Figs. 10a and 10b for specimen $R_6S_3T_1$ near the bifurcation point. The edge mode (Fig. 10b) corresponds to the back edge in Fig. 1, that is, an axial position of -152.4 mm (-6.00 in.). By comparison to the load-deflection behavior of this shell in the vicinity of bifurcation (Fig. 5), the local minima and maxima can be better understood. As shown in Fig. 10a, the center of the shell is noted to have an asymmetric (bifurcation) mode at a w_c/T_n value of 5.6, whereas in Fig. 10b, the asymmetric mode is not evident at the shell edge at a w_c/T_n value of 5.6, but is evident at a value of 6.6. By comparison to Fig. 5, the latter value of 6.6 corresponds to the first local minima. Thus, transition from the first local maxima (near a w_c/T_n value of 5.6) to the first minima (near a w_c/T_n value of 6.6) involves axial propagation of the asymmetric mode from the center to the free shell edges. Based on similar

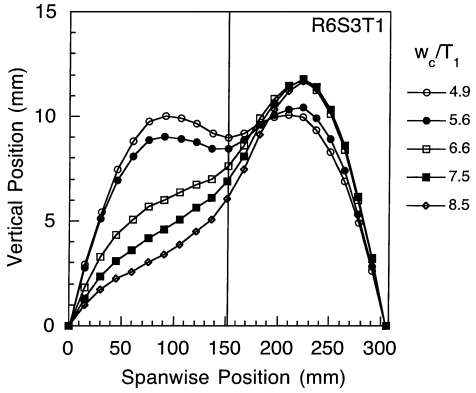

Fig. 10a Numerical results for spanwise deformation mode shapes at different normalized center deflections (w_c/T_1) near the bifurcation point for specimen $R_6S_3T_1$ at central axial location.

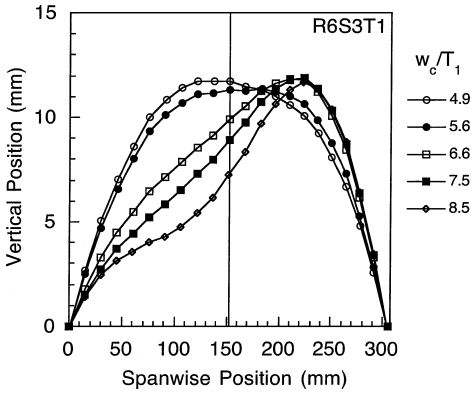

Fig. 10b Numerical results for spanwise deformation mode shapes at different normalized center deflections (w_c/T_1) near the bifurcation point for specimen $R_6S_3T_1$ at edge axial location.

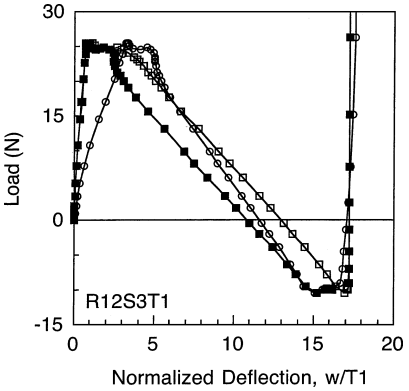

Fig. 11 Numerical results for load vs central and edge deflections for specimen $R_{12}S_3T_1$: ○, center; □, edge 1; and ■, edge 2.

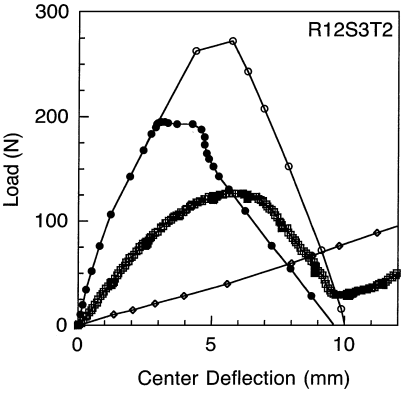

Fig. 12 Numerical and experimental[48] results for central load-deflection response for specimen $R_{12}S_3T_2$, radius = 1.677 m: ○, limit point; ●, bifurcation; □, data; and ◇, simple support.

considerations, the second local maxima (near a w_c/T_n value of 7.5) is seen in Fig. 10b to correspond to the shell edge deforming into a mode with an inflection point much like the central deformation mode. The local minima and maxima near the bifurcation point are, thus, explained by axial propagation of the asymmetric bifurcation mode from the shell center to the (free) shell edges.

The observation that the two free shell edges do not deform symmetrically throughout the entire shell response indicates a second two-dimensional aspect of the shell behavior. This second aspect of the two-dimensional shell response can be investigated by consideration of numerical force vs normalized center and edge deflections. This type of plot is presented in Fig. 11 for specimen $R_{12}S_3T_1$. Edge 1 corresponds to the back edge in Fig. 1 at an axial position of −152 mm (6.00 in.) and edge 2 corresponds to the front edge at an axial position of 152 mm (6.00 in.). Initially, both shell edges lag behind the response of the center of the shell, that is, at a given load, the shell center has greater deflection than the edges, but closely follow one another. Significant differences in the front and back edge responses are noted after the bifurcation point. The front edge is noted to lag behind the back edge through the bifurcation region. This behavior at the shell edges is due to the bending–twisting characteristic of the laminate. As the shell bends during loading, the laminate material coupling induces the shell to twist in the x–y shell plane, causing one shell edge to have a greater deformation than the other. Thus, due to bending–twisting coupling in the composite laminate, the two shell edges do not deform symmetrically (as in the isotropic benchmark problem). This twisting is evidenced in Figs. 9a and 9b as a slanting of the axial mode shapes and is discussed in Part 1 as axial slanting.[45] Thus, asymmetries in the composite shell response are due to bifurcation (asymmetric mode) and also due to bending–twisting material coupling in the composite laminate.

C. Experimental Realities

The measured responses of the composite shells are sensitive to imperfections and other experimental realities, such as nonideal boundary conditions,[32,52] indentation (contact modeling) at the loading point, and damage formation and propagation. These effects have not been accounted for in the elastic finite element models in this work. This is appropriate for many of the shells tested, such as those discussed in the preceding section, as illustrated by the excellent agreement between analysis and experiment. Thus, the point-load idealization of the indentor and the mathematical idealization of the hinged boundary condition are justified for specimens $R_6S_3T_1$ and $R_{12}S_3T_1$. Likewise, inevitable imperfections in the specimens and boundary conditions do not seem to affect the global response of these shells.

Results when all 18 specimens tested in Part 1 are modeled do indicate, however, that experimental realities, particularly boundary conditions, need to be considered in some cases.[45] These results show that, in general, the experimental load-deflection curves from Part 1 are more compliant than the predicted response. This has been attributed to compliance in the test fixture that interacts with the shell response through the hinged boundary condition.[32] Boundary conditions are known to be important in a general sense, but this is specifically the case in the response of thin composite shells,[32,52] and particularly when shell instabilities are involved.[53,54] Test fixture compliance of the kind considered in this work has been discussed by previous authors in relation to nonlinear collapse of arches at limit points.[51,55] Fixture compliance acts to soften the structural response and reduce, or even eliminate, limit points in arches.

In the experiments, because the load is introduced under deflection control, compliance of the test fixture in the direction of loading (z direction) is unimportant. However, compliance of the test fixture perpendicular to the applied loading will couple to the measured response. Compliance of the test fixture, thus, refers to the in-plane boundary condition of the hinged support. Rather than being fixed, as in the numerical idealization, there is a stiffness associated with the in-plane constraint. The compliant behavior of the experimental data relative to the numerical models is evident in Fig. 12, where numerical and experimental results are compared for specimen $R_{12}S_3T_2$. The predicted limit-point and bifurcation response of this shell are both observed to be much stiffer than the experimental results. This behavior can be attributed to test fixture compliance.

To investigate the magnitude of the test fixture compliance effect, a lower bound for the effect of the test fixture is considered when the shell is allowed to have a traditional simple support rather than a hinge in the finite element model. Thus, rather than being rigid (or fixed), the in-plane restraint is modeled as being free. In arch analyses, a simple support such as this allows the arch to deform continuously with no critical buckling load. The experimental response should, thus, lie between the two extremes of hinged and simply supported. This is in agreement with the results obtained for the shells analyzed here, as shown in Fig. 12. The simple support results are much more compliant than the hinged results and act as a lower bound to the measured response with regard to this aspect of the boundary condition. In reality, the test fixture will behave somewhere between a hinge and simple support, roughly acting as a spring in series with the stiffness of the shell. Analysis of all specimens tested in Part 1 shows that the hinged and simple support analyses generally bound the measured behavior.[45]

D. Implications for Damage Resistance

The numerical and experimental results discussed have implications for shell damage resistance studies. Bifurcation into asymmetric deformations, as observed here, suggests the possibility of asymmetric damage formation in composite shells. Asymmetric damage has been observed for transversely loaded composite shells[15,28] but is not a feature of plate response. Global deformation asymmetries will drive asymmetric stress states and may cause asymmetric damage formation, for example, the response of specimen $R_6S_3T_1$ shown in Figs. 7a and 7b could damage asymmetrically due to the asymmetric mode shapes. In such cases, the maximum curvature change

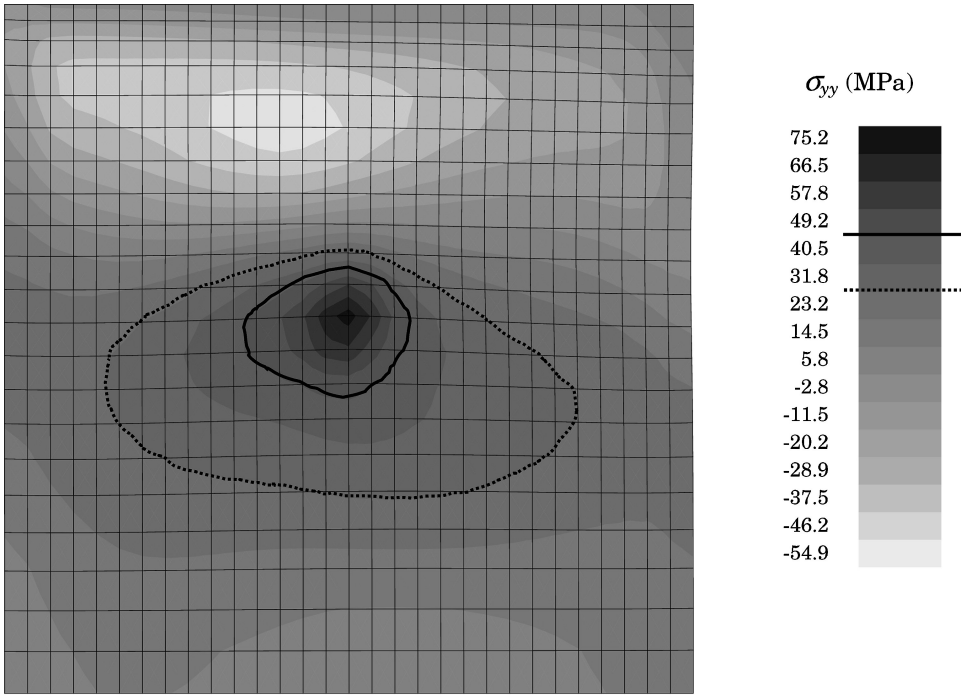

Fig. 13 Numerical model results for normal stress σ_{yy} contours in the bottom −45-deg ply plotted on the deformed geometry for specimen $R_6S_3T_1$ during postbuckling (postbifurcation) at a load of 50.5 N; σ_{yy} is the normal stress perpendicular to the fiber direction, that is, the normal ply matrix stress.

along the shell surface does not occur at the loading point, and, thus, the maximum bending stress can occur away from the loading point. This situation occurs as a result of the shell bifurcation under transverse loading and does not occur for plates.

The possibility of asymmetric damage formation is investigated by consideration of the stress state for a specimen that bifurcates. Normal stress perpendicular to the ply fibers at the back surface (concave shell surface) is presented in Fig. 13 for specimen $R_6S_3T_1$ at a load of 50.5 N in the post-bifurcated region of the load-deflection response. This ply stress is considered because transverse matrix cracks, attributable to this stress, are oftentimes observed on the back surface of damaged composite plates and shells. The tensile ply failure stress of approximately 50 MPa in the matrix direction for this material system is exceeded in an asymmetric region around the loading point (see detail in Fig. 13). The area where this stress is exceeded has the same shape as atypical damage states (matrix cracking and delamination) observed in previous work with composite shells for this laminate and material system.[15,28] The atypical and asymmetric damage states observed in previous work are likely due to bifurcation and the resultant asymmetric stress distribution.

Asymmetric damage distributions have not been previously observed in work with composite plates. Perhaps more importantly, asymmetric damage formation is also associated with increased damage extent relative to that observed for identical plates undergoing comparable transverse loadings.[45] Therefore, these observed asymmetric states associated with shell bifurcation warrant further investigation because plate damage resistance and tolerance investigations may not provide a conservative picture of shell response to damage and subsequent loading. Further work, such as an analysis that incorporates the global bifurcation behavior and local contact behavior, is suggested to elucidate damage formation in shell structures. Experimental damage tolerance investigations are also suggested to understand the effects, if any, of the atypical and asymmetric damage states observed for composite shells.

VI. Conclusions

The large-deflection buckling response of composite shell structures has been calculated by the use of the finite element method with a novel technique for the induction of bifurcation. The prebuckling, nonlinear collapse, bifurcation buckling, and postbuckling response of the laminated composite shells tested in Part 1,[45] and an isotropic benchmark problem, are accurately captured by the models. A full model with a rather coarse mesh involving only 110 elements is found to capture the composite response adequately, particularly bifurcation. Excellent agreement between the models and experiments is evident in load-deflection comparisons and, most convincingly, in deformation evolutions. In particular, specimen $R_6S_3T_1$ is seen as a useful benchmark for subsequent shell analyses given the excellent agreement between theory and experiment, including nonlinear prebuckling, bifurcation, and postbuckling. The novel AMT allows the bifurcation point and postbuckling to be accurately and efficiently evaluated when such behavior occurs, that is, the technique does not impose bifurcation, but rather finds it in the structural response if it exists. The two-dimensional nature of the shell response, as contrasted with a one-dimensional arch-type response, is elucidated by the numerical models. This two-dimensional response, along with asymmetries due to bifurcation and laminate material couplings, give rise to local minima and maxima in the load-deflection response near the bifurcation point. These local minima and maxima are found to be due to axial propagation of the bifurcation deformation mode of the shell.

The elastic analyses, and comparison with experimental data, clearly show that bifurcation must be considered in an evaluation of composite shell response: The critical load, deformation modes, and (likely) damage are significantly affected by bifurcation. An example of a typical fuselage structure, specimen $R_{12}S_2T_2$, bifurcates at 85% of the (symmetric) limit load in the numerical analyses, indicating that bifurcation must be included to assess this shell response accurately. Symmetric models typically used to analyze these types of shell problems cannot capture bifurcation and will yield inaccurate solutions.

Although bifurcation clearly needs to be considered for composite shells such as those considered herein, damage resistance is the ultimate aim of such modeling efforts. To understand, and even predict, damage formation will require much more sophisticated modeling efforts that include higher-order effects such as transverse shear. Further experimentation will also be necessitated: More careful experimental evaluation of boundary conditions and

methods of load introduction, as well as characterization (measurement) of structural imperfections are needed to characterize shell response, including buckling, more accurately. Damage characterization studies to characterize the onset and propagation of damage are needed. Further modeling efforts must consider higher-order effects not considered in the elastic models in this work. A primary concern, addressed in a preliminary sense in this work, is test fixture compliance that strongly couples to the shell response in this work. Likewise, higher-order models will need to address Hertzian contact loading, transverse shear, and scale effects. The elastic models presented in this work, with good agreement to experimental observations, provide a certain first step toward a coherent understanding of damage in laminated composite shell structures.

Acknowledgments

This work was sponsored by the Federal Aviation Administration under Research Grant 94-G-037 and NASA Langley Research Center under NASA Grant NAG-1-991.

References

[1]Amatore, D., "Composite Hydrogen Tank Test Completed for DC-XA," NASA News Press Release 96-13, Jan. 1996.

[2]Breivik, N. L., Gurdal, Z., and Griffin, O. H., "Compression of Laminated Composite Beams with Initial Damage," *Journal of Reinforced Plastics and Composites*, Vol. 12, No. 7, 1993, pp. 813–824.

[3]Chen, G.-S., Bidinger, G. M., and Lou, M. C., "Impact Damage in Small Diameter Graphite/Epoxy Composite Struts," *Proceedings of the 33rd AIAA/ASME/ASCE/AHS Structures, Structural Dynamics, and Materials Conference*, AIAA, Washington, DC, 1992, pp. 2945–2954.

[4]Abrate, S., "Impact on Laminated Composites: Recent Advances," *Applied Mechanics Review*, Vol. 47, No. 11, 1994, pp. 517–544.

[5]Abrate, S., "Impact on Laminated Composite Materials," *Applied Mechanics Review*, Vol. 44, No. 4, 1991, pp. 155–190.

[6]Cantwell, W. J., and Morton, J., "The Impact Resistance of Composite Materials," *Composites*, Vol. 22, No. 5, 1991, pp. 55–97.

[7]Kwon, Y. S., and Sankar, B. V., "Indentation-Flexure and Low-Velocity Impact Damage in Graphite Epoxy Laminates," *Journal of Composites Technology and Research*, Vol. 15, No. 2, 1993, pp. 101–111.

[8]Sjöblom, P. O., Hartness, J. T., and Cordell, T. M., "On Low-Velocity Impact Testing of Composite Materials," *Journal of Composite Materials*, Vol. 22, Jan. 1988, pp. 30–52.

[9]Lagace, P. A., Williamson, J. E., Tsang, P. H. W., Wolf, E., and Thomas, S., "A Preliminary Proposition for a Test Method to Measure (Impact) Damage Resistance," *Journal of Reinforced Plastics and Composites*, Vol. 12, No. 5, 1993, pp. 584–601.

[10]Lee, S., and Zahuta, P., "Instrumented Impact and Static Indentation of Composites," *Journal of Composite Materials*, Vol. 25, Feb. 1991, pp. 204–222.

[11]Jackson, W. C., and Poe, C. C., Jr., "The Use of Impact Force as a Scale Parameter for the Impact Response of Composite Laminates," *Journal of Composites Technology and Research*, Vol. 15, No. 4, 1992, pp. 282–289.

[12]Wu, E., and Shyu, K., "Response of Composite Laminates to Contact Loads and Relationship to Low-Velocity Impact," *Journal of Composite Materials*, Vol. 27, No. 15, 1993, pp. 1443–1464.

[13]Meyer, P. I., "Low-Velocity Hard-Object Impact of Filament-Wound Kevlar/Epoxy Composites," *Composite Science and Technology*, Vol. 33, No. 4, 1988, pp. 279–293.

[14]Manders, P. W., Bader, M. G., Hinton, M. J., and Flower, P. Q., "Mechanisms of Impact Damage in Filament Wound Glass-fibre/Epoxy-resin Tubes," *Third International Conference on Mechanical Behaviour of Materials*, Pergamon, Oxford, 1979, pp. 275–284.

[15]Wardle, B. L., and Lagace, P. A., "On the Use of Quasi-Static Testing to Assess Impact Damage Resistance of Composite Shells," *Mechanics of Composite Materials and Structures*, Vol. 5, No. 1, 1998, pp. 103–121.

[16]Kim, D., and Chaudhuri, R. A., "Full and Von Kármán Geometrically Nonlinear Analyses of Laminated Cylindrical Panels," *AIAA Journal*, Vol. 33, No. 11, 1995, pp. 2173–2181.

[17]Chang, T. Y., and Sawamiphakdi, K., "Large Deformation Analysis of Laminated Shells by Finite Element Method," *Computers and Structures*, Vol. 13, No. 1, 1981, pp. 331–340.

[18]Palazotto, A. N., Chien, L. S., and Taylor, W. W., "Stability Characteristics of Laminated Cylindrical Panels Under Transverse Loading," *AIAA Journal*, Vol. 30, No. 6, 1992, pp. 1649–1653.

[19]Ram, K. S. S., and Babu, T. S., "Buckling of Laminated Composite Shells Under Transverse Load," *Composite Structures*, Vol. 55, 2002, pp. 157–168.

[20]Kim, K., and Voyiadjis, G. Z., "Non-Linear Finite Element Analysis of Composite Panels," *Composites: Part B*, Vol. 30, 1999, pp. 365–381.

[21]Gummadi, L. N. B., and Palazotto, A. N., "Nonlinear Dynamic Finite Element Analysis of Composite Cylindrical Shells Considering Large Rotations," *AIAA Journal*, Vol. 32, No. 11, 1999, pp. 1489–1494.

[22]Gong, S. W., Shim, V. P. W., and Toh, S. L., "Impact Response of Laminated Shells with Orthogonal Curvatures," *Composites Engineering*, Vol. 5, No. 3, 1995, pp. 257–275.

[23]Ambur, D. R., and Starnes, J. H., Jr., "Nonlinear Response and Damage-Initiation Characteristics of Curved Composite Plates Subjected to Low-Speed Impact," *Proceedings of the 38th AIAA/ASME/ASCE/AHS/ASC Structures, Structural Dynamics, and Materials Conference*, AIAA, Reston, VA, 1997, pp. 1821–1831.

[24]Kim, S. J., Goo, N. S., and Kim, T. W., "The Effect of Curvature on the Dynamic Response and Impact-Induced Damage in Composite Laminates," *Composites Science and Technology*, Vol. 57, 1997, pp. 763–773.

[25]Krishnamurthy, K. S., Mahajan, P., and Mittal, R. K., "A Parametric Study of the Impact Response and Damage of Laminated Cylindrical Composite Shells," *Composites Science and Technology*, Vol. 61, 2001, pp. 1655–1669.

[26]Palazotto, A., Perry, R., and Sandhu, R., "Impact Response of Graphite/Epoxy Cylindrical Panels," *AIAA Journal*, Vol. 30, No. 7, 1992, pp. 1827–1832.

[27]Kistler, L. S., "Experimental Investigation of the Impact Response of Cylindrically Curved Laminated Composite Panels," *Proceedings of the 35th AIAA/ASME/ASCE/AHS/ASC Structures, Structural Dynamics, and Materials Conference*, AIAA, Washington, DC, 1994, pp. 2292–2297.

[28]Wardle, B. L., and Lagace, P. A., "Importance of Instability in Impact Response and Damage Resistance of Composite Shells," *AIAA Journal*, Vol. 35, No. 2, 1997, pp. 389–396.

[29]Lin, H. J., and Lee, Y. J., "Impact-Induced Fracture in Laminated Plates and Shells," *Journal of Composite Materials*, Vol. 24, Nov. 1990, pp. 1179–1199.

[30]Marshall, I. H., and Rhodes, J., "Snap-Buckling of Thin Shells of Rectangular Planform," *Stability Problems in Engineering Structures and Components*, edited by T. H. Richards and P. Stanley, Applied Science, London, 1979, pp. 249–264.

[31]Wardle, B. L., and Lagace, P. A., "Behavior of Composite Shells Under Transverse Impact and Quasi-Static Loading," *AIAA Journal*, Vol. 36, No. 6, 1998, pp. 1065–1073.

[32]Tudela, M. A., "Structural Response and Damage Development of Cylindrical Composite Panels," Technology Lab. for Advanced Composites, S. M. Thesis, TELAC Rept. 96-11, Dept. of Aeronautics and Astronautics, Massachusetts Inst. of Technology, Cambridge, MA, Sept. 1996.

[33]Johnson, E. R., Hyer, M. W., and Carper, D. M., "Response of Composite Material Shallow Arch to Concentrated Load," *Journal of Aircraft*, Vol. 123, No. 6, 1986, pp. 529–536.

[34]Bazant, Z. P., and Cedolin, L., *Stability of Structures: Elastic, Inelastic, Fracture, and Damage Theories*, Oxford Engineering Science Series, Oxford Univ. Press, New York, 1991, p. 984.

[35]Bushnell, D., *Computerized Buckling Analysis of Shells*, Mechanics of Elastic Stability, edited by H. H. E. Leipholz, and G. Æ. Oravas, Vol. 9, Martinus Nijhoff, Dordrecht, The Netherlands, 1985, pp. 1–28.

[36]Voyiadjis, G. Z., and Shi, G., "Nonlinear Postbuckling Analysis of Plates and Shells by Four-Noded Strain Element," *AIAA Journal*, Vol. 30, No. 4, 1992, pp. 1110–1116.

[37]Tsai, C. T., Palazotto, A. N., and Dennis, S. T., "Large-Rotation Snap-Through Buckling in Laminated Cylindrical Panels," *Finite Elements in Analysis and Design*, Vol. 9, No. 1, 1991, pp. 65–75.

[38]Saigal, S., Kapania, R. K., and Yang, T. Y., "Geometrically Nonlinear Finite Element Analysis of Imperfect Laminated Shells," *Journal of Composite Materials*, Vol. 20, March, 1986, pp. 197–214.

[39]Talbot, M., and Dhatt, G., "Three Discrete Kirchoff Elements for Shell Analysis with Large Geometrical Non-Linearities and Bifurcations," *Engineering Computations*, Vol. 4, March, 1987, pp. 15–22.

[40]Laschet, G., and Jeusette, J.-P., "Postbuckling Finite Element Analysis of Composite Panels," *Composite Structures*, Vol. 14, 1990, pp. 35–48.

[41]Simo, J. C., Fox, D. D., and Rifai, M. S., "Geometrically Exact Stress Resultant Shell Models: Formulation and Computational Aspects of the Nonlinear Theory," *Analytical and Computational Models of Shells*, edited by A. K. Noor, T. Belytschko, and J. C. Simo, American Society of Mechanical Engineers, New York, 1989, pp. 161–190.

[42]Noguchi, H., and Hisada, T., "Sensitivity Analysis in Post-Buckling Problems of Shell Structures," *Computers and Structures*, Vol. 47, No. 4/5, 1993, pp. 699–710.

[43]Crisfield, M. A., *Non-Linear Finite Element Analysis of Solids and Structures*, Vol. 1, Wiley, New York, 1991, pp. 268–269.

[44]Rankin, C. C., and Brogan, F. A., "An Element-Independent Corotational Procedure for the Treatment of Large Rotations," *Collapse Analysis of Structures: The 1984 Pressure Vessel and Piping Conference and Exhibition*, American Society of Mechanical Engineers, New York, 1984, pp. 85–100.

[45]Tudela, M. A., Lagace, P. A., and Wardle, B. L., "Buckling Response of Transversely Loaded Composite Shells, Part 1: Experiments," *AIAA Journal*, Vol. 42, No. 7, 2004, pp. 1457–1464.

[46]Wardle, B. L., "Buckling and Damage Resistance of Transversely-Loaded Composite Shells," Ph.D. Dissertation, Technology Lab. for Advanced Composites, TELAC Rept. 98-7, Dept. of Aeronautics and Astronautics, Massachusetts Inst. of Technology, Cambridge, MA, June 1998.

[47]Sabir, A. B., and Lock, A. C., "The Application of Finite Elements to the Large Deflection Geometrically Non-Linear Behaviour of Cylindrical Shells," *Variational Methods in Engineering*, edited by C. A. Brebbia and H. Tottenham, Vol. 2, Southampton Univ. Press, Surrey, England, U.K., 1973, pp. 7/66–7/75.

[48]Brogan, F. A., Rankin, C. C., Cabiness, H. D., and Loden, W. A., "STAGS User Manual—Version 2.3," Lockheed Martin Missiles and Space Co., Inc., LMMS PO32594, Palo Alto, CA, July 1996.

[49]Rankin, C., and Brogan, F., "The Computational Structural Mechanics Testbed Structural Element Processor ES5: STAGS Shell Element," NASA CR-4358, 1991.

[50]Riks, E., "Some Computational Aspects of the Stability Analysis of Nonlinear Structures," *Computer Methods in Applied Mechanics and Engineering*, Vol. 47, 1984, pp. 219–259.

[51]Timoshenko, S., *Theory of Elastic Stability*, Engineering Societies Monographs, McGraw–Hill, New York, 1936, pp. 204–238.

[52]Marshall, I. H., Rhodes, J., and Banks, W. M., "The Nonlinear Behaviour of Thin, Orthotropic, Curved Panels Under Lateral Loading," *Journal of Mechanical Engineering Science*, Vol. 19, No. 1, 1977, pp. 30–37.

[53]Arbocz, J., and Hol, J. M. A. M., "The Role of Experiments in Improving the Computational Models for Composite Shells," *Analytical and Computational Models of Shells*, edited by A. K. Noor, T. Belytschko, and J. C. Simo, American Society of Mechanical Engineers, New York, 1989, pp. 613–640.

[54]Arbocz, J., "Future Directions and Challenges in Shell Stability Analysis," *Proceedings of the 38th AIAA/ASME/ASCE/AHS/ASC Structures, Structural Dynamics, and Materials Conference*, AIAA, Reston, VA, 1997, pp. 1949–1962.

[55]Fung, Y. C., and Kaplan, A., "Buckling of Low Arches or Curved Beams of Small Curvature," NACA TN 2840, Nov. 1952.

E. R. Johnson
Associate Editor